Sensors & Transducers, Vol. 198, Issue 3, March 2016, pp. 55-60

Sensors & Transducers

http://www.sensorsportal.com

The Constrained Natural Element Method Applied in Electromagnetic Heterogeneous Models

[1] Bárbara Mara Ferreira GONÇALVES, [1] Marcio Matias AFONSO, [1] Eduardo Henrique da Rocha COPPOLI, [1] Ursula do Carmo RESENDE, [1] Sandro Trindade Mordente GONÇALVES, [2] Brahim RAMDANE, [2] Yves MARECHAL and [3] Christian VOLLAIRE

[1] Electrical Engineering Postgraduate Program - CEFET-MG - UFSJ, Minas Gerais, Brazil
[2] Electrical Engineering Laboratory of Grenoble – G2ELAB, Grenoble, France
[3] AMPERE Laboratory – Ecole Centrale de Lyon – ECL, Lyon, France
[1] Tel.: +55 (31) 3319-6841, fax: +55 (31) 3319-6724
[1] E-mail: marciomatias@des.cefetmg.br

Received: 11 February 2016 /Accepted: 14 March 2016 /Published: 31 March 2016

Abstract: In this paper the treatment of material discontinuities in the Natural Element Method (NEM) are discussed. A visibility criterion and the constrained Voronoï diagram are presented in order to take account this difficulty. The extension of NEM, the Constrained NEM (C-NEM), is applied to solve electromagnetic problems. An electrostatic problem is proposed and the approach is evaluated and compared with the traditional Finite Element Method (FEM). *Copyright © 2016 IFSA Publishing, S. L.*

Keywords: Material discontinuities, Natural element method, Visibility criterion, Constrained natural element method, Electromagnetism.

1. Introduction

With a great successful history, the Finite Element Method (FEM) is one of the most reputable numerical methods currently used as a reference in the numerical methods domain. However, despite its many advantages, the FEM also imposes difficulties in solving certain types of problems. In general, to solve problems involving the need of mesh reconstruction such as interfaces mobile or deformation with time, the Finite Element Method requires extensive computational and human effort.

In order to avoid numerical problems involving the construction of mesh the so-called meshless or mesh-free methods have been developed [1]. The meshless methods are increasingly being used in electromagnetic field computations [2-3]. In these methods a cloud of nodes without connectivity relations that covers the domain is used to solve the problem. Due to its characteristics, these methods are well suited to solve problems involving moving parts, like electrical machines [3-4].

It is well known that meshless methods provides high accuracy solutions but present some difficulties to handle boundary and interface conditions [4-5]. To eliminate these drawbacks, the natural element method (NEM) was proposed [6]. The NEM approach is based on the Voronoï diagram and the natural neighbors concept. The convergence of the NEM has been previously studied for different applications [2]. Also, the NEM main interest lies in its interpolation property which allows enforcing essential boundary

conditions and interface conditions in an easy way as with the FEM [2].

However, like other meshless methods, the NEM require special treatment in areas with different materials, i.e., in interfaces [6]. Many electromagnetic problems may involve heterogeneous media and therefore it is very important the proper treatment of discontinuity of material [7]. As this subject is not transparent for meshfree methods, the aim of this work is to discuss the treatment of material discontinuities in NEM and apply it to solve a classical electromagnetic problem.

2. Problem Formulation

For the purpose of analysis, consider the conductor strip of copper and aluminum shown by Fig. 1. The domain is characterized by $\Omega = \Omega_1 \cup \Omega_2$ and is desired to obtain the current distribution in both materials.

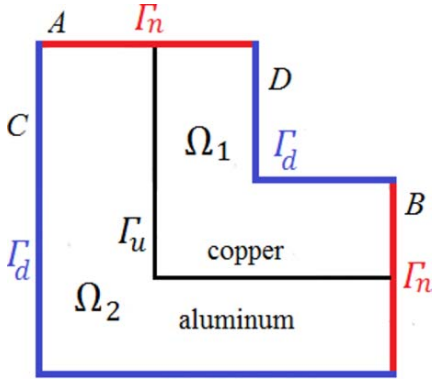

Fig. 1. Conductor strip (bimaterial domain) [8].

If a static current crosses Ω, the problem can be described by Laplace equation [8]:

$$\nabla.\left(\frac{1}{\sigma}\nabla T\right) = 0 \qquad (1)$$

$$T = I \text{ on } \Gamma_d \text{ and } \frac{\partial T}{\partial n} = 0 \text{ on } \Gamma_n \qquad (2)$$

(1) and (2) are the strong formulation of the problem where T is the electric potential vector and σ is the conductivity of the medium. Γ_n is the boundary with homogeneous Neumann condition formed by A and B lines, Γ_d is the boundary with Dirichlet boundary condition formed by the C and D lines, and Γ_u is the interface between sub-domains Ω_1 and Ω_2.

The discrete equation is obtained using the Galerkin method. So, the weak formulation can be written as:

$$\int_\Omega \frac{1}{\sigma}\nabla T^h \nabla w \, d\Omega = 0 \qquad (3)$$

In (3) Ω is the problem domain surrounded by the surface Γ (given by the lines A, B, C and D), T^h is an approximation for the scalar component of the electric potential vector T and w is the scalar weight function. Many numerical techniques can be used in the evaluation of (3). However, this paper is focused on NEM [6].

3. The Natural Element Method (NEM)

The natural element method uses the concept of natural neighbors which is based on the construction of Voronoï diagram on a cloud of nodes [6].

3.1. The Voronoï Diagram

In 2D, let consider a set of nodes $N = \{n_1, n_2, n_3, \cdots, n_N\}$ distributed in the whole domain Ω. The Voronoï diagram is a subdivision of the plane into regions V_i where each region V_i is associated with a node n_i, such that any point in V_i is closer to n_i than to any other node n_j with $j \neq i$. The regions V_i are the Voronoï cells of n_i. In mathematical terms, the Voronoï cell V_i is defined as [2]:

$$V_i = \{x \in \mathbb{R}^2 : d(x, x_i) < d(x, x_j) \; \forall \, j \neq i\}, \qquad (4)$$

where x_i is the coordinates of the node n_i and $d(x, x_j)$ the distance between node n_j and point x. Thus, V_i is the region of the plane that contains the points x closest to node n_i than to any other node in N. The construction of each Voronoï cell can be obtained by the intersection of the segments joining the node n_i to its neighbor nodes, and a straight line, normal to each one of these segments, traced at the central point of those segments [6].

This diagram subdivides the studied domain into a set of polygons which defines the natural neighbors of the node in its center. The Delaunay triangulation, which is the dual of the Voronoï diagram, is constructed by connecting the nodes whose Voronoï cells have common boundaries [2]. An important property of Delaunay triangles is the empty circumcircle criterion – there is no node inside the circumcircle of Delaunay triangle. In the context of natural neighbors interpolation these circles are known as natural neighbors circumcircles. The centre of the natural neighbor circumcircle is a vertex of the Voronoi cell. If the nodal set N is such that only three nodes lie on the circumcircle of any Delaunay triangle, then precisely three edges meet to form a Voronoi vertex [6].

The Voronoï diagram and Delaunay triangulation for a set N consisting of nine nodes are show in Fig. 2. The Voronoï cells V_1 e V_2 are highlighted and a circmcircle is illustrated. All nodes n_i are inside the called convex hull $CH(N)$. The convex hull of the set

of nodes N is the smallest convex set containing N. Note that the Voronoï cells are closed and convex, while the cells associated with nodes on the boundary of the convex hull are unbounded [6].

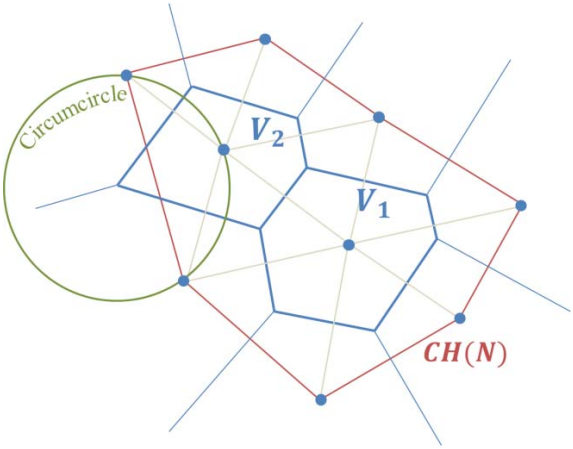

Fig. 2. Representation of Voronoï diagram (blue color), Delaunay triangulation (gray color), Voronoï cells V_1 and V_2, and the convex hull $CH(N)$.

From an algorithmic viewpoint, since the Voronoï diagram and the Delaunay triangulation share a common bond (duality), the combinatorial structure of either structure is completely determined from its dual.

The interpolation of a point can be obtained by introducing a fictitious point in the Voronoï diagram and calculating the value of the corresponding shape function.

3.2. The Shape Function

Based on the Voronoï diagram, the natural element shape function can be calculated. In the literature, several formulas are used to calculate this shape function [6]. Among the most used, are the Sibson functions which may be determined in analogy with classical FEM shape functions as the ratio of surfaces in the case of triangles [6]. The same principle is applied to Voronoï cells to achieve Sibson shape functions. A point x shown by Fig. 3(b) is inside Voronoï diagram of Fig. 3(a), so the Sibson shape function is given by (5) where each $S_i(x)$ represents the ratio of the subarea of Voronoï cell centered on x and linked to the natural neighbor n_i and the total area of Voronoï cell linked to that point $S(x)$ [6].

$$\phi_i(x) = \frac{S_i(x)}{S(x)}, \tag{5}$$

where i ranges from 1 to NV (number of natural neighbors visible from point x), and:

$$S(x) = \sum_{j=1}^{NV} S_j(x) \tag{6}$$

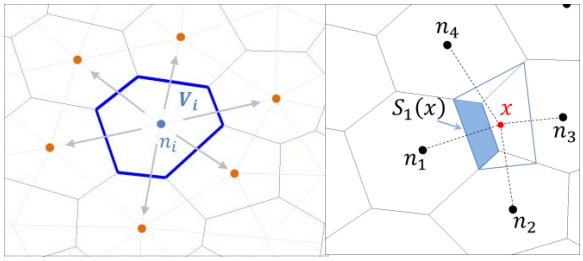

(a) (b)

Fig. 3. (a) The n_i node, its Voronoï cell T_i and its six natural neighbors. (b) NEM shape function computation where $S_1(x)$ represents the subarea associated with the node n_1.

The shape function in (5) is the natural neighbor coordinate (n-n coordinate). The derivatives of the natural coordinates are obtained by differentiating (5) [6]:

$$\phi_{i,j}(x) = \frac{S_{i,j}(x) - \phi_i S_{,j}(x)}{S(x)} \ (j = 1, 2) \tag{7}$$

3.3. Properties

The same properties of FEM are verified for NEM shape functions as positivity [2, 6]:

$$0 \le \phi_i(x) \le 1 \tag{8}$$

Kronecker delta (interpolation):

$$\phi_i(x_j) = \delta_{ij}, \tag{9}$$

partition of unity:

$$\sum_{i=1}^{NV} \phi_i(x) = 1 \tag{10}$$

and linear completeness:

$$x = \sum_{i=1}^{NV} \phi_i(x) x_i \tag{11}$$

Thus, the electric potential vector can be written as follows:

$$T^h(x) = \sum_{i=1}^{NV} T_i \phi_i(x), \tag{12}$$

where NV is the number of natural neighbor visible from point x and T^h is the approximation for the scalar component of the electric potential vector T.

By the circumcircle criterion, it is evident that for ϕ_i to have a non-zero contribution at x, the point x must lie within the circumcircle of a Delaunay triangle that has the node n_i as one of its vertices [5]. The support of ϕ_i (region in which $\phi_i > 0$) is the union of the circumcircles passing through the vertices of the Delaunay triangles containing the node n_i of Fig 3(a).

The support of a node n_i in a particular nodal distribution is depicted in Fig. 4. In the empty nodes $\phi_i = 0$, in the fill node $\phi_i = 1$ and in all blue surface $\phi_i > 0$.

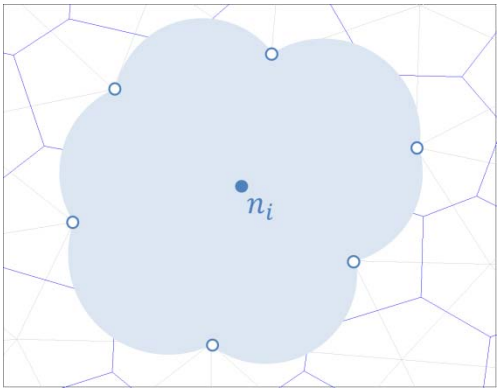

Fig. 4. Support of the natural shape function related to node n_i.

The final system of equations can be obtained by substituting the discrete form of trial and test functions (6) in (3) and applying it in all domain. After numerical integration, the following linear system of equation is obtained [8]:

$$KU = F, \tag{13}$$

where K is the global symmetric matrix, U is the unknown vector, and F is the source vector. The elements of the matrix K are given by:

$$K_{ij} = \int_{\Omega} \frac{1}{\sigma} \nabla\phi_j \, \nabla\phi_i \, d\Omega \tag{14}$$

4. Treatment of Material Discontinuities

Due to the inherent meshless characteristic, (6) can be computed in arbitrary clouds of nodes and these nodes can move freely on the background without any geometrical restriction [1-2]. In the interface between two regions of different materials (Γ_u), the FEM shape functions are linear completeness if the elements coincide with the Γ_u. In the NEM context, if Γ_u is straight the convex domain is hold and the shape functions along Γ_u are also linear. However, unlike FEM the nodes present in Ω_1 domain are influenced by nodes belonging to Ω_2 domain [7]. To treat the materials discontinuity a constrained Voronoï diagram associated with a visibility criterion is used [9-11].

4.1. The Visibility Criterion

The simplest way to solve the materials discontinuity lies in the introduction of a criterion to remove parasite influences between nodes on the interface Γ_u [9-10]. The point x is in the domain of influence of a node n_i if x is within the region where the shape function associated with n_i is non-zero ($\phi_i > 0$) and it is visible from node n_i when the boundaries are assumed opaque [9]. So, one can define [9]:

$$\Omega_i = \{x \mid x \in \Omega, \phi_i > 0\}, \tag{15}$$

$$\Omega_i^V = \left\{x \mid L_{x \to x_i} \cap \Gamma_u = \emptyset\right\}, \tag{16}$$

where $L_{x \to x_i}$ represents the straight line connecting x and n_i. Thus, the domain of influence of a node n_i, Ω_i^*, is defined as [9]:

$$\Omega_i^* = \Omega_i^V \cap \Omega_i \tag{17}$$

4.2. Constrained Voronoï Diagram

A constrained Voronoï diagram results from the application of the above criterion, which will be used to define the interpolation functions [9-10]. If a visibility criterion is applied on Γ_u the resulting Voronoï diagram is composed with cells V_i^C, one for each node n_i, such as any point x inside V_i^C is closer to n_i than to any other node n_j visible from x. It is called the constrained Voronoï cells, which are defined formally by [9]:

$$V_i^C = \Big\{x \in \mathbb{R}^2 : d(x, x_i) < d\big(x, x_j\big) \; \forall \, j \neq i, L_{x \to n_i} \cap \Gamma_u = \emptyset, L_{x \to n_j} \cap \Gamma_u = \emptyset\Big\} \tag{18}$$

Once such diagram is constructed, classical algorithms for the computation of the shape functions can be applied directly because connections between non-visible natural neighbors in different regions have been removed [9]. Based on the constrained Voronoï diagram, the constrained Natural Element Method (C-NEM) has been introduced [2, 10].

4.3. C-NEM Interpolation

If the visibility criterion is introduced in the NEM, the natural neighbors become constrained natural neighbors [9-10]. The set of natural neighbors will be restricted by applying the visibility criterion. Thus, the functional approximation for C-NEM can be written as [9]:

$$T^h(x) = \sum_{i=1}^{NV} T_i \phi_i^C(x), \tag{19}$$

where NV is the number of natural neighbors visible from point x and ϕ_i^C is the constrained natural neighbor shape function.

In C-NEM the support of ϕ_i^C is similar to ϕ_i for NEM interpolation consisting of the union of the circumcircles that pass through the vertices of the Delaunay triangles. However, these circumcircles can be extend across the boundaries, but cannot contain nonvisible neighbors [9].

In order to explain this, consider the node $n_\Gamma \in \Gamma_u$ showed in Fig. 1. The support of the constrained natural neighbor shape function ϕ_i^C associated to n_Γ is depicted in Fig. 5. In it, the subdomain Ω_1 has the support seen in Fig. 5(a) and the subdomain Ω_2 has the support showed in Fig. 5(b). Due to linearity of the C-NEM shape functions will assume the following values: $\phi_i^C = 0$ in the empty nodes, $\phi_i^C = 1$ in n_Γ (the filled node) and $\phi_i^C > 0$ in all blue surface.

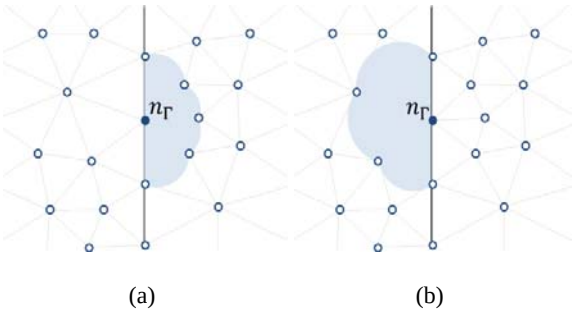

Fig. 5. Support of C-NEM shape functions associated with node n_Γ along Γ_u (a) in Ω_1 and (b) in Ω_2.

It can be shown that in the context of the constrained natural neighbors interpolation, any point in the domain lies inside the convex hull of their constrained (visible) natural neighbors. In consequence, the partition of unity and the linear consistency are conserved in the C-NEM [9]. Another important aspect is the fact that the influence between non-visible nodes has been removed during the construction of the constrained Voronoï diagram. In this case, influences of interior nodes also vanish. Thus, interface conditions can be easily enforced on any boundary where the approximation is in fact linear [9].

5. Results

Consider the structure showed at Fig. 1 to validate the proposed approach. A current difference is imposed between the lines C and D, such that $I_C = I_a$ and $I_D = 0$. I_a is the current flowing through the conductor.

Also, the width of the copper strip is chosen as the same as the aluminum one, $I_a = 1\frac{\text{A}}{\text{m}}$, $\sigma_{\text{copper}} = = 6{,}17\times10^7\ \text{S/m}$ and $\sigma_{\text{aluminum}} = 3{,}42\times10^7\ \text{S/m}$. Fig. 6 shows the resulting current distribution for a 125 nodes discretization using C-NEM. It could be observed that a higher current crosses the copper part of the conductor. Moreover, the current curve is smooth even close to the interface between the two mediums.

The result is also validated by comparison with the traditional FEM for the same discretization and plotted in Fig. 7. In this Figure the current distribution on dashed line A highlighted in Fig. 6 are compared. It can be observed a very good agreement between them. Also, is possible to see that the current in copper is approximately 60 % higher than the current in aluminum. This result is expected since the conductivity of copper is approximately 60 % higher than the conductivity of aluminum [8].

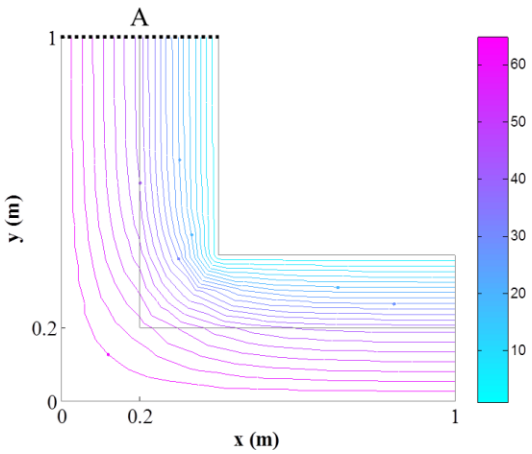

Fig. 6. Current distribution.

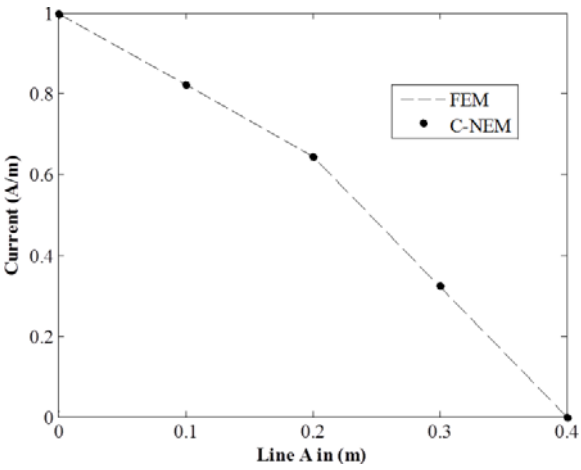

Fig. 7. Current along the line A depicted in Fig. 6.

For a better comparison of the aforementioned results, the relative error are obtained for NEM and FEM methods. The reference result is furnished by an extremely refined mesh (6273 nodes) of the FEM. The error is computed considering the L_2 norm of the solution vector T given as follows:

$$e = \sqrt{\int_\Omega \frac{(T-T_{ref})^2 d\Omega}{T_{ref}{}^2}}, \qquad (20)$$

where T_{ref} is the reference solution and Ω is the domain where the error is computed.

It is observed that the error committed by the C-NEM is less than the error made by FEM considering the same number of nodes. The ratio of the FEM and the NEM error is approximately 1.22. This result allow to verify that NEM is more accurate than FEM.

6. Conclusions

The treatment of interface condition in natural element method was adressed in this paper. The visibiliy criterion was discussed with details and C-NEM was applied to solve a bimaterial electromagnetic problem. The analysis of the solutions have demonstrated the applicability and accuracy of C-NEM to treat material discontinuities.

Acknowledgements

This work was partially supported by FAPEMIG, CAPES, CNPq and CEFET-MG.

References

[1]. T. Belytschko, Y. Krongauz, D. Organ, M. Fleming, P. Krysl, Meshless Methods: An Overview and Recent Developments, *Computer Methods in Applied Mechanics and Engineering*, Vol. 139, No. 1-4, 1996, pp. 3-47.

[2]. Y. Marechal, B. Ramdane, Natural Element Method Applied to Electromagnetic Problems, *Trans. on Magnetics*, Vol. 49, No. 5, May 2013, pp. 1713-1716.

[3]. L. Illoul, J. Yvonet, F. Chinesta, S. Clénet, Application of the Natural-Element Method to Model Moving Electromagnetic Devices, *IEEE Transactions on Magnetics*, Vol. 42. No. 4, 2006, pp. 727-730.

[4]. E. H. R. Coppoli, R. C. Mesquita, R. S. Silva, Periodic boundary conditions in element free Galerkin method, in *Proceedings of the International IGTE Symposium on Numerical Field Calculation in Electrical Engineering*, Graz, Austria, 2008, pp. 346-351.

[5]. Y. Marechal, B. Ramdane, D. P. Botelho, Computational Performances of Natural Element and Finite Element Methods, *IEEE Transactions on Magnetics*, Vol. 50, No. 2, 2014, pp. 68-73.

[6]. N. Sukumar, The Natural Element Method in Solid Mechanics, PhD dissertation, *Northwestern University*, USA, 1998.

[7]. B. M. F. Gonçalves, *et al.*, Treatment of material discontinuities in natural element method for electromagnetic problems, in *Proceedings of the XVII International Symposium on Electromagnetic Fields in Mechatronics, Electrical and Electronic Engineering*, Valencia, Spain, Sep. 2015.

[8]. Bastos J. P. A, Sadowski N., Electromagnetic Modeling by Finite Element Methods, *Marcel Dekker Inc.*, New York, 2003.

[9]. J. Yvonnet, D. Ryckelynck, P. Lorong, F. Chinesta, A new extension of the natural element method for non-convex and discontinuous domains: the constrained natural element method (C-NEM), *International Journal for Numerical Methods in Engineering*, Vol. 60, No. 8, 2004, pp. 1451-1474.

[10]. J. Yvonnet, *et al.*, The constrained natural element method (C-NEM) for treating thermal models involving moving interfaces, *International Journal of Thermal Sciences*, Vol. 44, No. 6, 2005, pp. 559-569.

[11]. B. M. F. Gonçalves, *et al.*, Periodic Boundary Conditions in the Natural Element Method, *IEEE Transactions on Magnetics*, Vol. 52, No. 3, 2015, pp. 1-4.